

## Effectiveness of induced magnetic force and non-uniform heat source/sink features for enhancing the thermal efficiency of third grade nanofluid containing microorganisms

Yun-Jie Xu<sup>a</sup>, Sami Ullah Khan<sup>b</sup>, Kamel Al-Khaled<sup>c</sup>, M. Ijaz Khan<sup>d,e</sup>,  
Faris Alzahrani<sup>e</sup>, M. Imran Khan<sup>f,\*</sup>

<sup>a</sup> School of Engineering, Huzhou University, Huzhou, 313000, PR China

<sup>b</sup> Department of Mathematics, COMSATS University Islamabad, Sahiwal, 57000, Pakistan

<sup>c</sup> Department of Mathematics & Statistics, Jordan University of Science and Technology, P.O. Box 3030, Irbid, 22110, Jordan

<sup>d</sup> Department of Mathematics and Statistics, Riphah International University, I-14, Islamabad, 44000, Pakistan

<sup>e</sup> Nonlinear Analysis and Applied Mathematics (NAAM) Research Group, Department of Mathematics, Faculty of Science, King Abdulaziz University, P.O. Box 80257, Jeddah, 21589, Saudi Arabia

<sup>f</sup> CECOS University of IT & Emerging Sciences, Peshawar, Pakistan

### ARTICLE INFO

#### Keywords:

Third grade nanofluid  
Induced magnetic force  
Non-uniform heat generation/absorption  
Numerical scheme

### ABSTRACT

Owing to the multidisciplinary significance and dynamic applications of nanoparticles, the research in areas of thermal and process engineering has been expanding every day. The nano-materials with extraordinary thermal and physical properties are being studied to pose some astonishing contributions in various fields. The nanomaterials when taken with microorganisms in a solution for collective transport, referred as mix fluids, greatly improve the thermal efficiency during heat transfer phenomena. Usually, the mixed fluids particles have greater advantage of being controlled by some physical stimuli of light, gravity and density along with electrical and magnetic forces. The current study offers some innovative applications of induced magnetic field for the bio-convection pattern third grade nanofluid under the influence of extraordinary activation energy and non-uniform heat source/sink factors. The assumptions of stagnation points are considered under the influence of stretched. The nano-materials have been mixed with micro-organism to prepare a mixed fluid in order to obtain more stability and directed transportation. The flow constraints for the thermal transport phenomenon have been explained by using convective boundary approach. The couple and nonlinear equations have been put forward to present the model and the solution has been derived using shooting algorithm technique. Moreover, the numerical and graphical outcomes from the study are presented using tables and figures. The improved profile of velocity is predicted against higher values of velocity ratio, Reynolds number and third grade fluid parameter. The induced magnetic field profile enhanced for reciprocal magnetic Prandtl number and magnetic parameter. The consideration of non-uniform heat source/sink is more effective to improve and control and thermal transportation process.

\* Corresponding author. University of Portsmouth School of Engineering University of Portsmouth, Portsmouth, United Kingdom.  
E-mail addresses: [muhammad.khan4@myport.ac.uk](mailto:muhammad.khan4@myport.ac.uk), [imrankhan@cecos.edu.pk](mailto:imrankhan@cecos.edu.pk) (M.I. Khan).

<https://doi.org/10.1016/j.csite.2021.101305>

Received 11 July 2021; Received in revised form 28 July 2021; Accepted 30 July 2021

Available online 3 August 2021

2214-157X/© 2021 Published by Elsevier Ltd. This is an open access article under the CC BY-NC-ND license

(<http://creativecommons.org/licenses/by-nc-nd/4.0/>).

## 1. Introduction

This century has been an era of scientific exploration of high efficiency, thermally active and exceptionally stable nanomaterials that are point of research these days. The nanomaterials when suspended in a solution have made an excellent contribution to the science of nuclear studies, heating and cooling of electro-mechanical devices, fission and fusion, thermal engineering and mass flow. Due to the extremely unique applications in science and engineering the nanoparticles have been selected to contribute towards more national energy sector in developing countries. When compared with base fluids like water and oils the nanomaterial suspended solutions have added advantages of high heat and mass transfer, increased thermophysical properties and improved stability. These parameter are the milestones that have underwritten vast applications of nanofluids in biotechnology, renewable energy, drug delivery, pharmaco-kinetics and all engineering disciplines including aviation and mechatronics. Choi [1] has been the pioneer who initially reported the properties of nanoparticle along with experimental support data. The improved heat transfer studies accompanying induced magnetic field were presented by Wakif et al. [2]. The investigation of improved parameters of Oldroyd-B nanofluid was performed by Khan et al. [3] under the influence of radiation via Prandtl approach. The stability of nanoparticles and hydrodynamic application of the nanofluids were exploited by Turkyilmazoglu [4]. The investigations conducted by Ibrahim [5] included the behavior of Maxwell nanofluid in features of uniform induced magnetic force. The thermal aspects of micropolar fluids through porous surface with induced magnetic field were investigated by Shehzad et al. [6]. Anisotropic slip studies for nanoparticles under the magnetic effect were reported by Nadeem et al. [7]. The explorations of Ikram et al. [8] were focused on enhancing thermal distribution pattern of hybrid nanofluids. Hosseinzadeh et al. [9] reported an exclusive improvement in heat transfer for model of cross nanofluids in three dimensions. The analysis of shrinking/stretching conditions of spongy surface immersed in hybrid nano-suspension was predicted by Khan and investigators [10]. The thermal model proposed by Salehi et al. [11] pronounced the role of variable magnetic forces on nanofluid flow through parallel plates. The viscoelastic nanofluid thermal effectiveness for Darcy-Forchheimer over a periodically moving surface was directed by Li et al. [12]. The investigations of an exponentially accelerated curved plate immersed in nanofluid were led by Wahid et al. [13]. Gowda et al. [14] presented the inspired features of magnetic dipole for the Stefan blowing flow of ferromagnetic nanoparticles codified by stretching surface. Kumar et al. [15] inspected the aspects of thermodiffusion prospective while addressing the flow of ferromagnetic nanofluid. Gowda et al. [16] used the modified relations of Cattaneo-Christov to predict the fluctuation in heat and mass phenomenon for Sutterby nanofluid. The rotating flow analysis for hybrid nanofluid with magnetic force impact was characterized by Reddy et al. [17]. Yusuf et al. [18] determined the entropy generation consequences for the Williamson nanofluid flow over inclined surface. Acharya [19] successfully implemented the spectral quasi numerical scheme for present the solution of nanofluidic transport problem with multiple convective constraints. Acharya and Mabood [20] determined the comprehensive thermal change in the thermal transport of base fluid by using the  $\text{Fe}_3\text{O}_4$ -graphene hybrid nanoparticles. The hybrid nanofluid flow due to texture in presence of radiative phenomenon has been described by Acharya et al. [21].

The themes of bioconvection are related with microscopic suspending particles flow that accompany heat and mass transfer at large and uplift base fluid properties. The density of nanofluid is key parameter that influences the bioconvection patterns even when microorganisms are mixed. The density stratification leads the movement of suspended fluid particles (nanoparticles/microbes) in a way that sometimes the particles move anti gravimetrically due to high density lower layers. These density strata determine the stability of the fluid particles and the net gyrotactic bioconvection scheme. Bioconvection has been found to have many applications in the fields of renewable energy where biofuels production reactors, solar panel plates, microbial fuel cell and syn-gas technology. The biotechnology science has also been benefitted by bioconvection studies that have revolutionized the targeted drug delivery, biosensor devices, integrated metabolism, nanomedicine, nano-catalysis, pyrolysis and anaerobic digestion. Engineering and geology has also been benefitted by bioconvection studies with its applications in microsystems, mining and drilling, polymer science, robotics, oil extraction and refineries. The bioconvection studies of nanoparticles as solution were performed by Kuznetsov [22,23]. The constraints of blowing features and slip were investigated by Uddin et al. [24] with a special focus on variable buoyant forces. Imran et al. [25] addressed the bioconvection applications for nanofluid flow under the influence of magnetic dipole. Acharya et al. [26] presented the effects of solar radiation over nanofluid bioconvection. The exploration of Eyring-Powell nanofluid flow with slip effects and the numerical estimation was done by Anas et al. [27]. The analysis conducted by Khan et al. [28] reported the problems that were posed in by thixotropic fluids of mixed nature. Acharya et al. [29] exploited the properties of chemically reactive material and studied the slip effects and squeezing bioconvection pattern. Khan et al. [30] investigated the activation energy features of micropolar nanofluid along with gyrotactic microorganisms. An off centered moving disk submerged in micropolar nanofluid with extraordinary thermal assets was studied by Song et al. [31].

The activation energy is another novel research topic for scientists. The basic idea and definition activation energy was directed in 1889 by Arrhenius. Activation energy predicts the supplied energy amount to the reactants in any chemical process for initialing the process. The kinetic energy along with potential energy assigned to the molecules to break the bonding. The applications of activation energy include industries of oil storage, oil suspensions, geothermal systems and hydrodynamics [32–35].

The literature that has been reviewed spans the pioneer to advanced research in bioconvection studies. This theoretical communication aims to present the contribution of induced magnetic impact for bio-convective third grade nanofluid flow in presence of activation energy. The features of non-uniform heat source/sink are also attributed to suggest the thermal applications. It is remarked that much attention has been paid by researchers for the bioconvection flow of nanoparticles under different flow situations. However, the applications of bioconvection phenomenon for third grade non-Newtonian fluid under the inspired features of induced magnetic force have not been investigated yet. The choice of third grade fluid is interesting as this model presents the shear thinning and shear thickening rheological features more effectively [36,37]. The novel importance of induced magnetic impact regarding the bio-convective transport is visualized in solar energy and thermal engineering like extrusion processes, heat exchangers, energy

production, cooling of microchips, nuclear systems, transportation processes etc. Refs [38–41]. represents different flow aspects over a stretched surfaces.

### 2. Flow model

The study considered the flow of third grade nanoparticles under the influence of strong magnetic field and stagnation point analysis for 2-D flow. Stability of nanoparticles is confirmed by examination of nanofluid in presence of microorganisms. The linear change in fluid particle movement is observed at surface  $y = 0$ . The model development was performed by assuming steady flow of nanofluid while following Cartesian coordinates. The representation of plate velocity over the moving sheet and free stream regime is respectively represented as  $u = ax$  and  $u = bx$ , where  $a$  and  $b$  are representatives of stretching velocity coefficients. Convective mass flux and constraints are employed to analyze convective transport. The magnetic field induction has been take as normal to the flow surface.  $H_1$  and  $H_2$  are the respective representations of magnetic components along horizontal and normal surface. Its noteworthy remarked that induced magnetic component  $H_2$  is along normal direction vanishes near the flow surface while parallel component  $H_1$  asymptotically close to  $H_0$ . The velocity components along normal and horizontal space is defined by  $v$  and  $u$ , respectively. The free stream zone concentration, motile density and temperature are denoted with  $c_\infty$ ,  $n_\infty$  and  $T_\infty$ , respectively. Following such constraints, the modeled equations are [5, 36, 37]:

$$\frac{\partial u}{\partial x} + \frac{\partial v}{\partial y} = 0, \tag{1}$$

$$\frac{\partial H_1}{\partial x} + \frac{\partial H_2}{\partial y} = 0, \tag{2}$$

$$u \frac{\partial u}{\partial x} + v \frac{\partial u}{\partial y} = \nu \frac{\partial^2 u}{\partial y^2} + \frac{\alpha_1^*}{\rho_f} \left[ \begin{aligned} &v \frac{\partial^3 u}{\partial y^3} + \frac{\partial u}{\partial x} \frac{\partial^2 u}{\partial y^2} \\ &+ u \frac{\partial^3 u}{\partial x \partial y^2} + \frac{\partial u}{\partial y} \frac{\partial^2 v}{\partial y^2} \end{aligned} \right] + \frac{6\beta_3}{\rho_f} \left( \frac{\partial u}{\partial y} \right)^2 \frac{\partial^2 u}{\partial y^2} - \frac{\sigma B_0^2}{\rho_f} u + u_\infty \frac{\partial u_\infty}{\partial x} + \mu_e \frac{dU_e}{dx} \tag{3}$$

$$- \frac{\mu}{4\pi\rho_f} H_e \frac{\partial H_e}{\partial x} + \frac{\mu}{4\pi\rho_f} \left( H_1 \frac{\partial H_1}{\partial x} + H_2 \frac{\partial H_1}{\partial y} \right) - \left\{ \begin{aligned} &(\rho_p - \rho_f)(c - c_\infty)g \\ &+ g(1 - c_\infty)g\alpha\rho_f(T - T_\infty) \\ &- (n - n_\infty)\nabla\rho\gamma g \end{aligned} \right\},$$

$$u \frac{\partial H_1}{\partial x} + v \frac{\partial H_2}{\partial y} = H_1 \frac{\partial u}{\partial x} + H_2 \frac{\partial u}{\partial y} + u_e \frac{\partial^2 H_1}{\partial x^2}, \tag{4}$$

$$u \frac{\partial T}{\partial x} + v \frac{\partial T}{\partial y} = \frac{k_f}{(\rho c)_f} \frac{\partial^2 T}{\partial y^2} + \tau_T \left[ D_T \frac{\partial C}{\partial y} \frac{\partial T}{\partial y} + \frac{D_T}{T_\infty} \left( \frac{\partial T}{\partial y} \right)^2 \right] + \frac{Q}{(\rho c)_f},$$

where non-uniform heat source/sink factor  $Q$  is:

$$Q = \frac{KU_w}{\nu} (A_1(T_f - T_\infty)f' + B_1(T - T_\infty)), \tag{5}$$

$$u \frac{\partial C}{\partial x} + v \frac{\partial C}{\partial y} + Kr^2(C - C_\infty) \left( \frac{T}{T_\infty} \right)^m \exp\left( \frac{-E_a}{k_a T} \right) = \frac{D_T}{T_\infty} \frac{\partial^2 T}{\partial y^2} + D_B \frac{\partial^2 C}{\partial y^2}, \tag{6}$$

$$u \frac{\partial N}{\partial x} + v \frac{\partial N}{\partial y} + \frac{b_m w_m}{(c_w - c_\infty)} \frac{\partial}{\partial y} \left( N \frac{\partial C}{\partial y} \right) = D_m \frac{\partial^2 N}{\partial y^2}, \tag{7}$$

The boundary conditions are [5]:

$$u = ax, v = 0, \frac{\partial H_1}{\partial y} = H_2 = 0, -k \frac{\partial T}{\partial y} = h_f(T_f - T), C = C_w, N = N_w \quad \text{at } y = 0, \tag{8}$$

$$u \rightarrow u_\infty = bx, \frac{\partial u}{\partial y} \rightarrow 0, H_1 = H_e(x) \rightarrow H_0(x), T \rightarrow T_\infty, C \rightarrow C_\infty, N \rightarrow N_\infty \text{ at } y \rightarrow \infty. \tag{9}$$

where  $\alpha_1^*$  and  $\beta_3$  symbolized the material constants for third grade nanofluid. The remaining are physical quantities are density  $\rho_f$ , volume expansion coefficient  $\alpha$ , electric conductivity  $\sigma$ , diffusion coefficient  $D_B$ ,  $x$ - magnetic component edge at boundary  $H_e$ , thermophoretic coefficient  $D_T$ , heat capacity nanofluid ratio  $\tau_w$ , Boltzmann constant  $\kappa^*$ , rate constant  $m$ , microorganisms diffusion  $D_m$ , Stefan Boltzmann constant  $\sigma^*$ , activation energy  $E_a$ , nanoparticles density  $\rho_p$ , gravity  $g$ , cell densities difference  $\nabla\rho$ , reaction constant  $Kr$ , chemotaxis constant  $b_m$ , average volume of microorganism  $\gamma$  and swimming cells speed  $w_m$ .

The transformations are [5]:

$$\left. \begin{aligned} v &= -\sqrt{av}f(\eta), H_2 = -H_0\sqrt{\frac{\nu}{a}}s(\eta), \eta = \sqrt{\frac{a}{\nu}}y, u = axf'(\eta), \\ \varphi(\eta) &= \frac{C - C_\infty}{C_w - C_\infty}, \theta(\eta) = \frac{T - T_\infty}{T_f - T_\infty}, \chi(\eta) = \frac{N - N_\infty}{N_w - N_\infty}. \end{aligned} \right\} \tag{10}$$

Utilizing these transformations in governing equations results:

$$f''' - f'^2 + ff'' + B^2 + \varepsilon(l^2 - ll'' - 1) + \alpha[2f'f'' - ff''' - f''^2] + 6\beta Re f''^2 f''' + Gr(\theta - Nr\varphi - Rb\chi) = 0, \tag{11}$$

$$A(l''' - lf'' + f''') = 0, \tag{12}$$

$$\frac{1}{Pr}\theta'' + f\theta' + Nb\theta'\varphi' + Nt(\theta')^2 + A_1f' + B_1\theta = 0, \tag{13}$$

$$\varphi'' + \left(\frac{Nt}{Nb}\right)\theta'' - Sc\sigma_c(1 + \omega\theta)^m \exp\left(-\frac{E}{1 + \omega\theta}\right)\varphi + Scf\varphi' = 0, \tag{14}$$

$$\chi'' - Pe\{(\sigma_m + \chi)\varphi'' + \chi'\varphi'\} + Lbf\chi' = 0. \tag{15}$$

with boundary conditions:

$$f(0) = 0, f'(0) = 1, l(0) = l''(0) = 0, \theta'(0) = -Bi[1 - \theta(0)], \varphi(0) = 1, \chi(0) = 1, \tag{16}$$

$$f'(\infty) \rightarrow B, f''(\infty) \rightarrow 0, l'(\infty) \rightarrow 1, \theta(\infty) \rightarrow 1, \varphi(\infty) \rightarrow 1, \chi(\infty) \rightarrow 1. \tag{17}$$

with velocity ratio ( $B$ ), material parameters ( $\alpha, \beta$ ), Reynolds number ( $Re$ ), mixed convection parameter ( $Gr$ ), buoyancy ratio constant ( $Nr$ ), Rayleigh number ( $Rb$ ), reciprocal magnetic Prandtl number ( $A$ ), Prandtl number ( $Pr$ ), magnetic parameter ( $\varepsilon$ ), Brownian constant ( $Nb$ ), activation energy ( $E$ ), thermophoresis constant ( $Nt$ ), Lewis number ( $Le$ ), bio-convective Lewis number ( $Lb$ ), Peclet number ( $Pe$ ) and motile difference constant ( $\sigma_m$ ).

$$\begin{aligned} B &= \frac{b}{a}, \alpha = a\alpha_1^* / \mu, \beta = \beta_3 a^2 / \mu, Re = ax^2 / \nu, Nr = \frac{\nabla\rho m(C_w - C_\infty)}{\alpha\rho_f(1 - c_\infty)(T_f - T_\infty)}, \varepsilon = \frac{\mu}{4\pi\rho_f} \left(\frac{H_0}{a}\right)^2, A = \frac{\mu_e}{\nu}, E = E_a / k_a T_\infty, \\ Gr &= \frac{gm(1 - c_\infty)(T_f - T_\infty)}{\nu^2}, Nb = \frac{\tau_w D_B(C_w - C_\infty)}{\alpha_m}, Pr = \frac{\nu}{\alpha_m}, Le = \frac{\alpha_m}{D_B}, Rb = \frac{\nabla\rho(n_w - n_\infty)}{\alpha\rho_f(1 - c_\infty)(T_f - T_\infty)}, Nt = \frac{\tau_w D_T(T_w - T_\infty)}{T_\infty \alpha_m}, Lb = \frac{\alpha_m}{D_m}, \\ Pe &= \frac{b_m w_m}{D_m}, \sigma_m = \frac{n_\infty}{(n_w - n_\infty)} \end{aligned}$$

The heat, mass and motile density rates are evaluated with help of following quantities:

$$\left. \begin{aligned} (Re_x)^{-1/2} Nu &= -\theta'(0), \\ (Re_x)^{-1/2} Sh &= -\varphi'(0), (Re_x)^{-1/2} Nn = -\chi'(0). \end{aligned} \right\} \tag{18}$$

### 3. Numerical scheme

The solution process is followed with implementations of shooting numerical method by using the MATLAB software. The suggested employed transformations to develop the problem in terms of first order system is:

$$\left. \begin{aligned} f &= r_1, f' = r_2, f'' = r_3, f''' = r_4, f'' = r_4', l = r_5, l' = r_6, l'' = r_7, l''' = r_7', \\ \theta &= r_8, \theta' = r_9, \theta'' = r_9', \varphi = r_{10}, \varphi' = r_{11}, \varphi'' = r_{12}, \chi = r_{13}, \chi' = r_{14}, \chi'' = r_{14}'. \end{aligned} \right\} \tag{19}$$

The transformed form of system is:

$$r_4' = \frac{r_4 - r_2^2 + r_1 r_3 + B^2 + \varepsilon(r_6^2 - r_5 r_7 - 1) + \alpha_1 [2r_1 r_4 - r_3^2] + 6\beta Re r_3^2 r_4 + Gr(r_8 - (Nr)r_{10} - Rbr_{13})}{\alpha_1 r_1}, \tag{20}$$

$$r_7' = \frac{r_5 r_3 + r_1 r_7}{A}, \tag{21}$$

$$r_9' = -Pr(r_1 r_9 + Nbr_9 r_{11} + Nt(r_9)^2 + A_1 r_2 + B_1 r_8), \tag{22}$$

$$r_{11}' = -Scq_1 q_{11} - \frac{Nt}{Nb} r_8' + Sc\sigma^{**} (1 + \delta r_7)^n r_{11} \exp\left(\frac{-E}{1 + \delta r_{11}}\right), \tag{23}$$

$$r_{14}' = r_1 r_{14} - Lbr_1 r_9 + Pe(r_{13} + \varpi) r_{12}. \tag{24}$$

With

$$r_1(0) = 0, r_2(0) = 1, r_5(0) = r_7(0) = 0, r_9(0) = -Bi[1 - r_8(0)], r_{11}(0) = 1, r_{13}(0) = 1, \tag{25}$$

$$r_2(\infty) \rightarrow B, r_3(\infty) \rightarrow 0, r_6(\infty) \rightarrow 1, r_8(\infty) \rightarrow 1, r_{11}(\infty) \rightarrow 1, r_{13}(\infty) \rightarrow 1. \tag{26}$$

By using the iterative process, the results are inspected with accuracy of  $10^{-7}$ .

#### 4. Discussion

The numerical simulated data for parameters is visualized physically in this section. Fig. 1(a) is a representation of variation in velocity  $f'$  due to changing third grade parameters  $\alpha$  and  $\beta$ . The escalating change in both  $\alpha$  and  $\beta$  resulted the inclining velocity profile. The explanation in Fig. 1(b) represents an increasing evolution for  $f'$  for higher velocity ratio  $B$  and magnetic parameter  $\epsilon$ . The explanation of buoyant forces is related with mixed convection parameters. The results indicated that maximum change in  $f'$  is due to higher variation of  $\epsilon$  and  $B$ . Fig. 2(a) observed the physical appliances of bioconvection Rayleigh number  $Rb$  and third grade fluid  $\alpha$  parameter induced magnetic field  $\tilde{l}$ . A leading enhancement in  $\tilde{l}$  is noted for  $Rb$ . This increasing trend is physically justified with involvement of bioconvection buoyancy forces. However, a suppressed nature of  $\tilde{l}$  is observed with distinct increasing values of  $\alpha$ . The increasing interpretation of induced magnetic profile is visualized against reciprocal magnetic Prandtl constant  $A$  and magnetic constant  $\epsilon$  in Fig. 2(b).

Fig. 3(a) is an illustrative of effects on temperature profile  $\theta$  by variation in material parameter  $\alpha$  and Reynolds number  $Re$ . The value of  $\theta$  have been found to show a decrement when  $\alpha$  and  $Re$  are maximum. The relationships and effects of buoyancy parameter  $Nr$  and magnetic parameter  $\epsilon$  on  $\theta$  are drafted using Fig. 3(b). The value of  $\theta$  is found climbing when growing buoyancy parameter  $Nr$ . The insight physical appliances for this profile is related to the bioconvection buoyancy forces due to  $Nr$ . With increasing change in magnetic parameter  $\epsilon$ ,  $\theta$  also enhanced. Fig. 3(d) clarifies the relationship of  $A_1$  and  $B_1$  on  $\theta$ . It can be seen that increasing values of both parameters the boost the temperature profile. Fig. 3(c) depicts the impact of thermophoresis parameter  $Nt$  and Brownian motion constant  $Nb$  on temperature  $\theta$ . A increasing contribution in nanofluid temperature is observed for  $Nt$  and  $Nb$ . The thermophoretic phenomenon involves the movement of heat nanoparticles from an area of higher temperature to lower on the surface that help to lift the net temperature of a system.

The enrolment of buoyancy parameter  $Nr$  and reciprocal magnetic Prandtl  $A$  on  $\varphi$  are presented in Fig. 4(a). A hint of decrease is observed for  $\varphi$  when  $A$  attains the numerical output. However, a boosted profile of  $\varphi$  is inspected for  $Nr$ . This boosted nature of concentration is attributed to the presence of buoyancy forces due to bioconvection. The nanoparticles concentration presents a diminishing change due to leading values of  $Nb$  and Reynolds number  $Re$  (see Fig. 4(b)). Fig. 4(c) presents how nanofluid concentration  $\varphi$  is affected by varying activation energy  $E$  and thermophoresis constant  $Nt$ . The higher values of both parameters were found associated with rapid rise in  $\varphi$ . The increasing change in concentration due to  $E$  is justified as activation effectively enhanced the chemical reaction process. Moreover, the concentration profile also rises against  $Nt$  due to the thermophoresis phenomenon.

The physical explanation presented in Fig. 5(a) notified the change in microorganisms profile  $\chi$  due to bio-convective Lewis constant  $Lb$  and Peclet parameter  $Pe$ . The declining profile of  $\chi$  is inspected for  $Pe$  which is justified due to inverse relations of Peclet constant with motile diffusivity. Moreover,  $\chi$  also declined with  $Lb$ . Fig. 5(b) reports the leading Prandtl number  $A$  and buoyancy ratio constant  $Nr$  on microorganism's profile. An increasing and reducing change in  $\chi$  has been observed for  $Nr$  and  $A$ , respectively.

The numerical change due to parameters for  $-f''(0)$  is noticed in Table 1. The increasing numerical values due to  $\alpha$  and  $Re$  are noticed. The flow parameters like  $\epsilon$ ,  $A$  and  $Rb$  presents a contradictory trend. Table 2 evaluates the numerical evaluation of  $-\theta'(0)$ ,  $-$

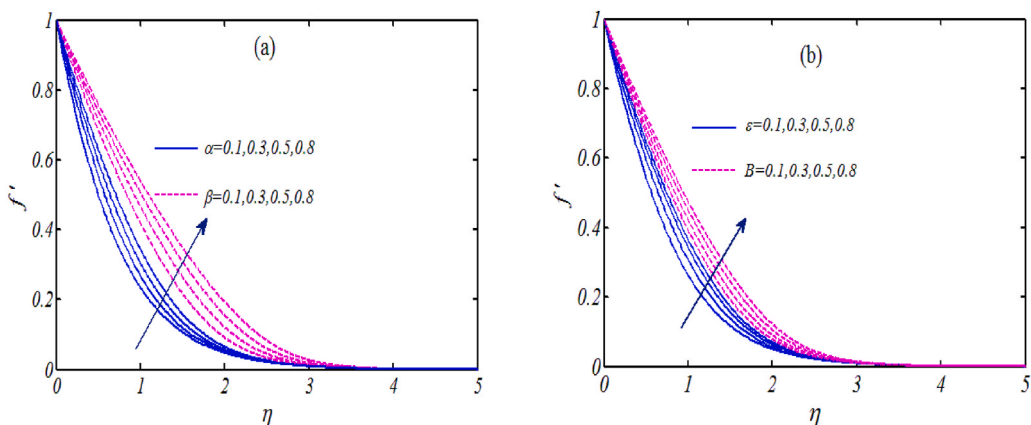


Fig. 1. Velocity profile for (a)  $\alpha$  and  $\beta$  (b)  $\epsilon$  and  $B$ .

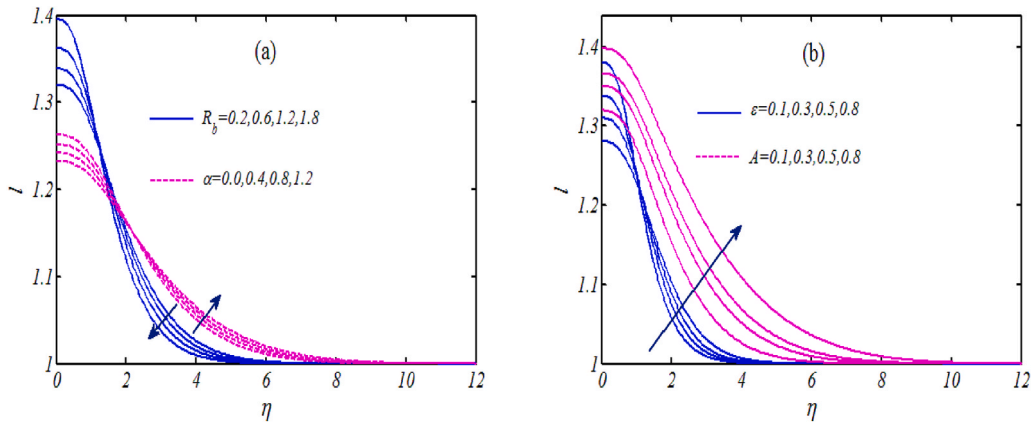


Fig. 2. Induced magnetic field for (a)  $\alpha$  and  $R_b$  (b)  $\epsilon$  and  $A$ .

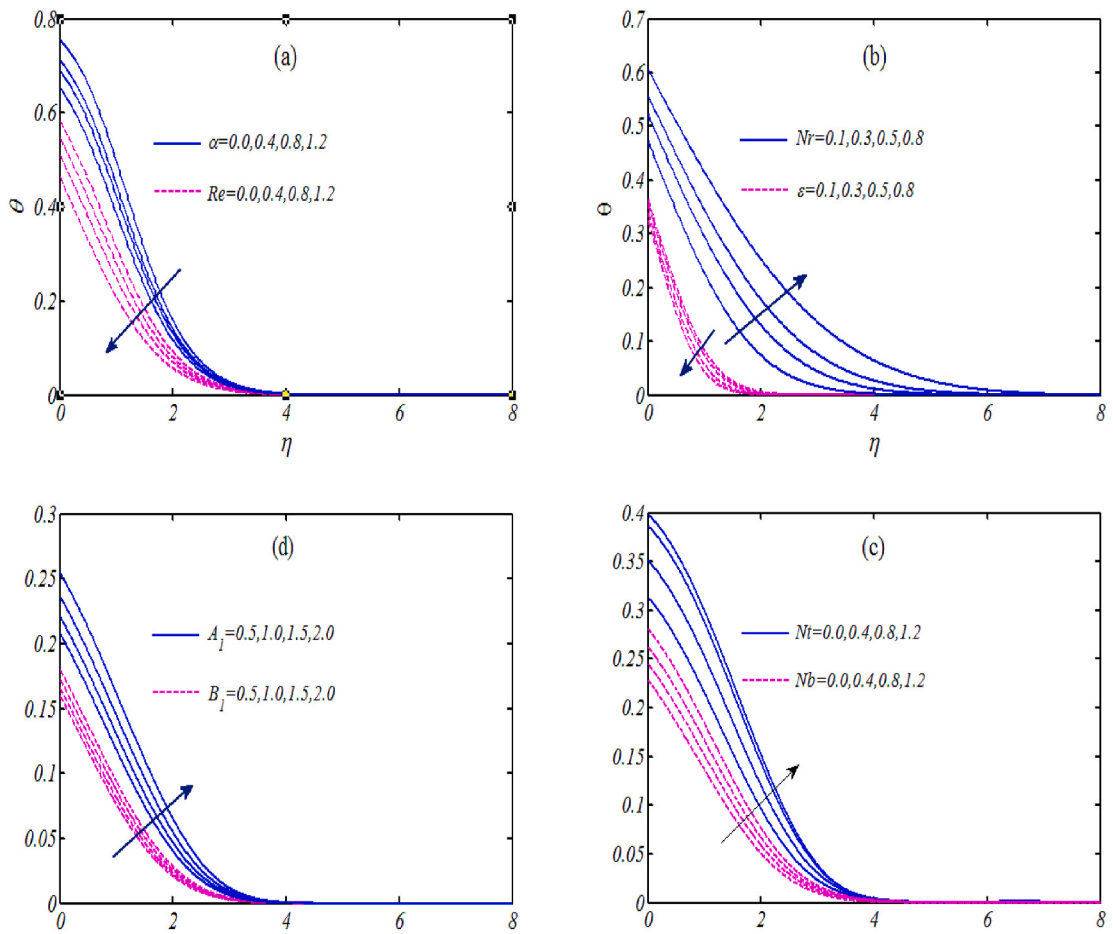


Fig. 3. Temperature profile for (a)  $\alpha$  and  $Re$  (b)  $\epsilon$  and  $Nr$ , (d)  $A_1$  and  $B_1$  (c)  $Nt$  and  $Nb$ .

$\phi'(0)$  and  $-\chi'(0)$  for parameters. The gradually rise in physical quantities is noted for  $\delta Gr$  and  $Pr$ .

### 5. Conclusions

The applications of induced magnetic force, non-uniform heat source/sink and activation energy are theoretically inspected for third grade nanofluid. The numerical outcomes are obtained via shooting technique. The novel outcomes are:

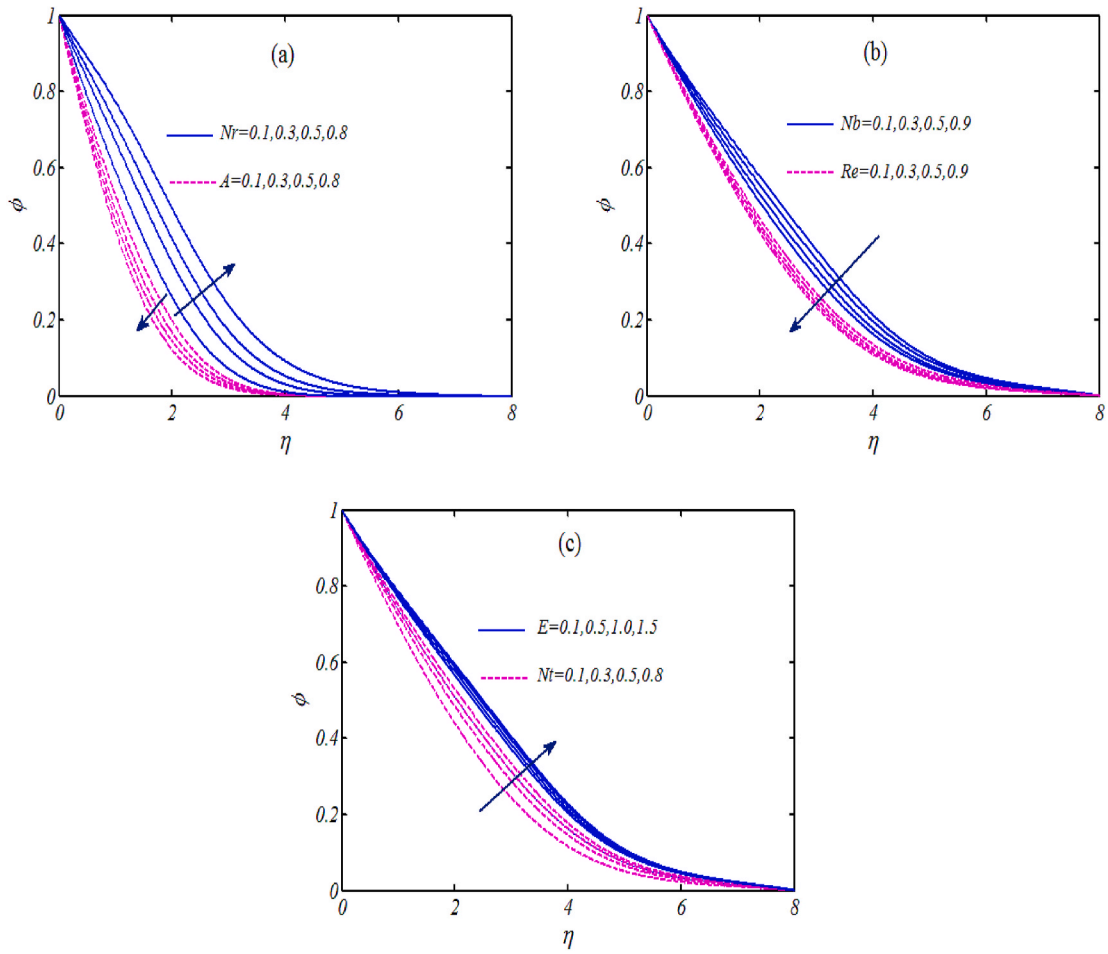


Fig. 4. Concentration profile for (a)  $Nr$  and  $A$  (b)  $Re$  and  $Nb$  and (c)  $Nt$  and  $E$ .

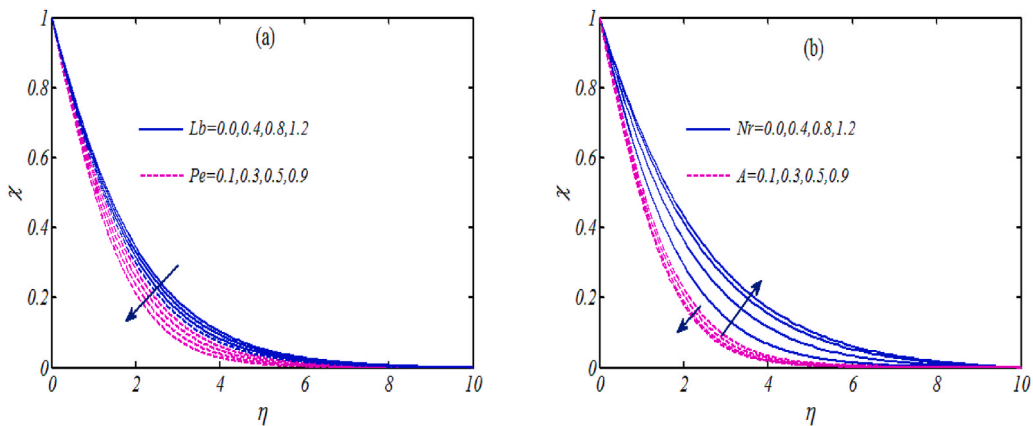


Fig. 5. Microorganisms profile for (a)  $Lb$  and  $Pe$  (b)  $Nr$  and  $A$ .

- ❖ The peak change in velocity is observed for third grade fluid parameter and velocity ratio constant.
- ❖ In increasing effects of fluid parameter is obtained for induced magnetic field profile.
- ❖ The reciprocal magnetic Prandtl number and magnetic parameter enhanced the induced magnetic field profile.
- ❖ The third grade fluid parameter and Reynolds number sufficiently improves the temperature profile.
- ❖ The valuable contribution of uniform heat source phenomenon is observed and result an increasing change in heat transfer rate.

**Table 1**  
Numerical change in  $-f''(0)$  for parameters.

$\alpha$	Re	$\varepsilon$	A	Gr	Rb	$-f''(0)$
0.1	0.2	0.4	0.2	0.2	0.4	0.44467
0.5						0.47853
0.7						0.53175
	0.3					0.45785
	0.7					0.47587
	0.9					0.49602
		0.01	0.4	0.2	0.4	0.43320
		0.03				0.42741
		0.05				0.41857
		0.2	0.3			0.45259
			0.7			0.44748
			1.1			0.44504
				0.1		0.47408
				0.5		0.46377
				0.7		0.45149
					0.1	0.44584
					0.5	0.38305
					0.9	0.366711

**Table 2**  
Numerical change in  $-\theta'(0)$ ,  $-\varphi'(0)$  and  $-\chi'(0)$ .

$\delta$	A	Gr	Rb	Pr	$-\theta'(0)$	$-\varphi'(0)$	$-\chi'(0)$
0.01	0.2	0.4	0.2	0.8	0.38748	0.29748	0.4567
0.03					0.35526	0.27285	0.43659
0.05					0.31325	0.255965	0.39238
0.2	0.3				0.41748	0.315748	0.410478
	0.7				0.37629	0.265128	0.38291
	1.1				0.32674	0.2473858	0.35759
		0.1			0.39525	0.357784	0.44917
		0.5			0.35774	0.328658	0.42369
		0.7			0.32085	0.287857	0.39851
			0.1		0.44529	0.414748	0.48965
			0.5		0.42737	0.37298	0.45857
			0.9		0.38698	0.315368	0.42748
				0.1	0.374299	0.44452	0.41775
				0.7	0.317687	0.37147	0.35405
				1.3	0.260756	0.284857	0.31754

- ❖ The concentration shows declining nature with Reynolds number and reciprocal magnetic Prandtl number.
- ❖ The microorganism profile enhanced when reciprocal magnetic Prandtl number is maximum.
- ❖ The current flow model results can be further modified and extended for different non-Newtonian fluids like Jeffrey fluid, Oldroyd-B fluid, Casson fluid, Burgers fluid, couple stress fluid etc. Moreover, this analysis will become more interesting for consideration of entropy generation features.

**Author statement**

All authors are equally contributed in this research work.

**Declaration of competing interest**

The authors declare that they have no known competing financial interests or personal relationships that could have appeared to influence the work reported in this paper.

**Acknowledgement**

This work was supported by the Zhejiang Province welfare technology applied research project (Grant No.: LGN21C160008).

## References

- [1] S.U.S. Choi, Enhancing thermal conductivity of fluids with nanoparticles, ASME-Publications-Fed 231 (1995) 99–106.
- [2] A. Wakif, Z. Boulaiah, S.R. Mishra, M.M. Rashidi, R. Sehaqui, Influence of a uniform transverse magnetic field on the thermo-hydrodynamic stability in water-based nanofluids with metallic nanoparticles using the generalized Buongiorno's mathematical model, Eur. Phys. J. Plus 133 (5) (2018) 181.
- [3] Sami Ullah Khan, A. Rauf, Sabir Ali Shehzad, Z. Abbas, T. Javed, Study of bioconvection flow in Oldroyd-B nanofluid with motile organisms and effective Prandtl approach, Phys. Stat. Mech. Appl. 527 (2019). Article No. 121179.
- [4] M. Turkyilmazoglu, Single phase nanofluids in fluid mechanics and their hydrodynamic linear stability analysis, Comput. Methods Progr. Biomed. 187 (2020) 105171.
- [5] W. Ibrahim, The effect of induced magnetic field and convective boundary condition on MHD stagnation point flow and heat transfer of upper-convected Maxwell fluid in the presence of nanoparticle past a stretching sheet, Propuls. Power Res. 5 (2) (2016) 164–175.
- [6] Sabir Ali Shehzad, Sami Ullah Khan, Z. Abbas, A. Rauf, A revised Cattaneo-Christov micropolar viscoelastic nanofluid model with combined porosity and magnetic effects, Appl. Math. Mech. 41 (2020) 521–532.
- [7] S. Nadeem, Muhammad Israr-ur-Rehman, S. Saleem, Ebenezer Bonyah, Dual solutions in MHD stagnation point flow of nanofluid induced by porous stretching/shrinking sheet with anisotropic slip, AIP Adv. 10 (2020), 065207.
- [8] Muhammad Danish Ikram, Muhammad Imran Asjad, Akgül Ali, Baleanu Dumitru, Effects of hybrid nanofluid on novel fractional model of heat transfer flow between two parallel plates, Alexandria Eng. J. 60 (Issue 4) (August 2021) 3593–3604.
- [9] Kh Hosseinzadeh, So Roghani, A.R. Mogharrebi, A. Asadi, M. Waqas, D.D. Ganji, Investigation of cross-fluid flow containing motile gyrotactic microorganisms and nanoparticles over a three-dimensional cylinder, Alexandria Eng. J. 59 (Issue 5) (October 2020) 3297–3307.
- [10] Umair Khan, Iskandar Waini, Anuar Ishak, Ioan Pop, Unsteady hybrid nanofluid flow over a radially permeable shrinking/stretching surface, J. Mol. Liq., Volume 331, 1 June 2021, 115752.
- [11] Sajad Salehi, Amin Nori, Kh Hosseinzadeh, D.D. Ganji, Hydrothermal analysis of MHD squeezing mixture fluid suspended by hybrid nanoparticles between two parallel plates, Case Stud. Thermal Eng. ume 21 (October 2020) 100650.
- [12] Li Yi-Xia, Kamel Al-Khaled, Sami Ullah Khan, Tian-Chuan Sun, M. Ijaz Khan, M.Y. Malik, Bio-convective Darcy-Forchheimer periodically accelerated flow of non-Newtonian nanofluid with Cattaneo-Christov and Prandtl effective approach, Case Stud. Thermal Eng. 26 (August 2021) 101102.
- [13] Nur Syahirah Wahid, Norihan MdArifin, Najiyah Safwa Khashi'ie, Ioan Pop, Norrifah Bachok, Mohd Ezad Hafidz Hafidzuddin, Flow and heat transfer of hybrid nanofluid induced by an exponentially stretching/shrinking curved surface, Case Stud. Thermal Eng., Volume 25, June 2021, 100982.
- [14] R.J. Punith Gowda, R. Naveen Kumar, B.C. Prasannakumara, B. Nagaraja, B.J. Gireesha, Exploring magnetic dipole contribution on ferromagnetic nanofluid flow over a stretching sheet: an application of Stefan blowing, J. Mol. Liq. 335 (1) (2021) 116215.
- [15] R Naveen Kumar, R.J. Punith Gowda, G.D. Prasanna, B.C. Prasannakumara, Kottakkaran Sooppy Nisar, Wasim Jamshed, Comprehensive study of thermophoretic diffusion deposition velocity effect on heat and mass transfer of ferromagnetic fluid flow along a stretching cylinder, Proc. IME E J. Process Mech. Eng. (2021), <https://doi.org/10.1177/09544089211005291>.
- [16] R.J. Punith Gowda, R. Naveen Kumar, A. Rauf, B.C. Prasannakumara, S.A. Shehzad, Magnetized flow of sutterby nanofluid through cattaneo-christov theory of heat diffusion and stefan blowing condition, Appl. Nanosci. (2021), <https://doi.org/10.1007/s13204-021-01863-y>.
- [17] M Gnaneswara Reddy, R. Naveen Kumar, B.C. Prasannakumara, N.G. Rudraswamy, K. Ganesh Kumar, Magneto-hydrodynamic flow and heat transfer of a hybrid nanofluid over a rotating disk by considering Arrhenius energy, Commun. Theor. Phys. 73 (2021), 045002.
- [18] Tunde A. Yusuf, Fazle Mabood, B.C. Prasannakumara, Ioannis E. Sarris, Fluids, Magneto-bioconvection flow of Williamson nanofluid over an inclined plate with gyrotactic microorganisms and entropy generation 6 (3) (2021) 109.
- [19] Nilankush Acharya, Spectral quasi linearization simulation of radiative nanofluidic transport over a bended surface considering the effects of multiple convective conditions, Eur. J. Mech. B Fluid 84 (2020) 139–154. November–December.
- [20] Nilankush Acharya, Fazle Mabood, On the hydrothermal features of radiative Fe<sub>3</sub>O<sub>4</sub>-graphene hybrid nanofluid flow over a slippery bended surface with heat source/sink, J. Therm. Anal. Calorim. 143 (2021) 1273–1289.
- [21] Nilankush Acharya, Bag Raju, Prabir Kumar Kundu, On the impact of nonlinear thermal radiation on magnetized hybrid condensed nanofluid flow over a permeable texture, Appl. Nanosci. 10 (2020) 1679–1691.
- [22] A.V. Kuznetsov, The onset of nanofluid bioconvection in a suspension containing both nanoparticles and gyrotactic microorganisms, Int. Commun. Heat Mass Tran. 37 (10) (2010) 1421–1425.
- [23] A.V. Kuznetsov, Nanofluid bioconvection in water-based suspensions containing nanoparticles and oxytactic microorganisms: oscillatory instability, Nanoscale Res. Lett. 6 (2011) 100.
- [24] Md JashimUddin, M.N. Kabir, O. Anwar Beg, Computational investigation of Stefan blowing and multiple-slip effects on buoyancy-driven bioconvection nanofluid flow with microorganisms, Int. J. Heat Mass Tran. 95 (April 2016) 116–130.
- [25] Muhammad Imran, Umar Farooq, Taseer Muhammad, Sami Ullah Khan, Waqas Hassan, Bioconvection transport of Carreau nanofluid with magnetic dipole and nonlinear thermal radiation, Case Stud. Thermal Eng. 26 (2021) 101129.
- [26] Nilankush Acharya, Kalidas Das, Prabir Kumar Kundu, Framing the effects of solar radiation on magneto-hydrodynamics bioconvection nanofluid flow in presence of gyrotactic microorganisms, J. Mol. Liq. 222 (October 2016) 28–37.
- [27] Anas M. Alwatban, Sami Ullah Khan, Waqas Hassan, Iskander Tlili, Interaction of Wu's slip features in bioconvection of Eyring Powell nanoparticles with activation energy, Processes 7 (11) (2019) 859.
- [28] M. Ijaz Khan, Fazal Haq, Sohail A. Khan, T. Hayat, M.Imran Khan, Development of thixotropic nanomaterial in fluid flow with gyrotactic microorganisms, activation energy, mixed convection, Comput. Methods Progr. Biomed. 187 (April 2020) 105186.
- [29] Nilankush Acharya, Bag Raju, Prabir Kumar Kundu, Unsteady bioconvective squeezing flow with higher-order chemical reaction and second-order slip effects, Heat Tran. Asian Res. (2021), <https://doi.org/10.1002/hjt.22137>.
- [30] M. Ijaz Khan, Waqas Hassan, Sami Ullah Khan, Muhammad Imran, Yu-Ming Chu, Ammar Abbasi, Seifedine Kadry, Slip flow of micropolar nanofluid over a porous rotating disk with motile microorganisms, nonlinear thermal radiation and activation energy, Int. Commun. Heat Mass Tran. 122 (2021) 105161.
- [31] Ying-Qing Song, ShanAli Khan, Muhammad Imran, Waqas Hassan, Sami Ullah Khan, M. Ijaz Khan, Sumaira Qayyum, Yu-Ming Chu, Applications of modified Darcy law and nonlinear thermal radiation in bioconvection flow of micropolar nanofluid over an off centered rotating disk, Alexandria Eng. J. 60 (Issue 5) (October 2021) 4607–4618.
- [32] R. Kalaivanan, N. Vishnu Ganesh, Qasem M. Al-Mdallal, An investigation on Arrhenius activation energy of second grade nanofluid flow with active and passive control of nanomaterials, Case Stud. Thermal Eng. 22 (2020) 100774. December.
- [33] Z. Nisar, T. Hayat, A. Alsaedi, B. Ahmad, Significance of activation energy in radiative peristaltic transport of Eyring-Powell nanofluid, Int. Commun. Heat Mass Tran. 116 (July 2020) 104655.
- [34] Samaira Aziz, Iftikhar Ahmad, Sami Ullah Khan, Nasir Ali, A three-dimensional bioconvection Williamson nanofluid flow over bidirectional accelerated surface with activation energy and heat generation, Int. J. Mod. Phys. B 35 (09) (2021) 2150132, 2021.
- [35] Zhao-Wei Tong, Sami Ullah Khan, Hanumesh Vaidya, Rajashekhar Rajashekhar, Tian-Chuan Sun, M. Ijaz Khan, K.V. Prasad, Ronnason Chinram, Ayman A. Aly, Nonlinear thermal radiation and activation energy significances in slip flow of bioconvection of Oldroyd-B nanofluid with Cattaneo-Christov theories, Case Stud. Thermal Eng. 26 (August 2021) 101069.
- [36] Yu-Ming Chu, M. Ijaz Khan, Niaz B. Khan, Seifedine Kadry, Sami Ullah Khan, Iskander Tlili, M.K. Nayak, Significance of activation energy, bio-convection and magnetohydrodynamic in flow of third grade fluid (non-Newtonian) towards stretched surface: a Buongiorno model analysis, Int. Commun. Heat Mass Tran. 118 (November) (2020) 104893.

- [37] Mouna Ben Henda, Waqas Hassan, Mohib Hussain, Sami Ullah Khan, Wathek Chammam, Shan Ali Khan, Iskander Tlili, Applications of activation energy along with thermal and exponential space-based heat source in bioconvection assessment of magnetized third grade nanofluid over stretched cylinder/sheet, *Case Stud. Thermal Eng.* ume 26 (August 2021) 101043.
- [38] M.I. Khan, M.Z. Kiyani, M.Y. Malik, T. Yasmeen, M.W.A. Khan, T. Abaas, Numerical investigation of magnetohydrodynamic stagnation point flow with variable properties, *Alexandria Eng. J.* 55 (2016) 2367–2373.
- [39] T. Hayat, M.I. Khan, M. Waqas, A. Alsaedi, On Cattaneo–Christov heat flux in the flow of variable thermal conductivity Eyring–Powell fluid, *Res. Phys.* 7 (2017) 446–450.
- [40] J. Wang, R. Muhammad, M.I. Khan, W.A. Khan, S.Z. Abbas, Entropy optimized MHD nanomaterial flow subject to variable thicked surface, *Comput. Methods Progr. Biomed.* 189 (2020) 105311.
- [41] M. Ibrahim, M.I. Khan, Mathematical modeling and analysis of SWCNT-Water and MWCNT-Water flow over a stretchable sheet, *Comput. Methods Progr. Biomed.* 187 (2020) 105222.